AD-A166 600 DAYTIME AND NIGHTTIME NEUTRAL WIND AND TEMPERATURE MEASUREMENTS FROM INCO.. (U) AIR FORCE INST OF TECH WRIGHT-PATTERSON AFB OH L O BELSMA DEC 85 1/1

UNCLASSIFIED AFIT/CI/NR-86-33T F/G 4/1 NL

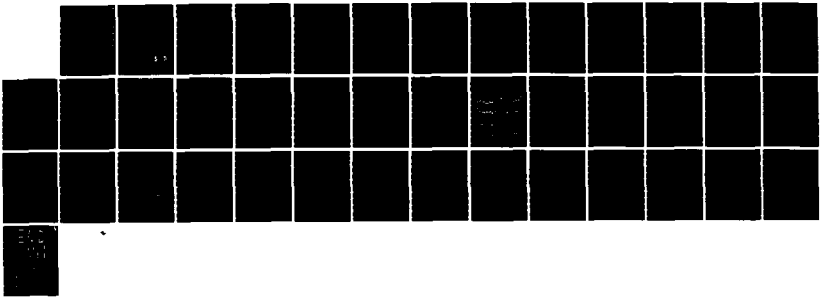

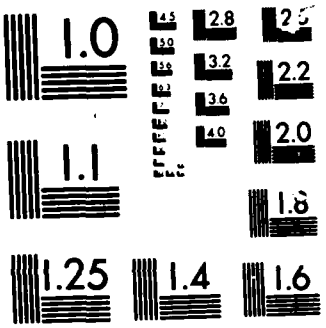

MICROCOPY CHART

AD-A166 600

SECURITY CLASSIFICATION OF THIS PAGE (When Data Entered)

REPORT DOCUMENTATION PAGE		READ INSTRUCTIONS BEFORE COMPLETING FORM
1. REPORT NUMBER AFIT/CI/NR 86- 33T	2. GOVT ACCESSION NO	3. RECIPIENT'S CATALOG NUMBER
4. TITLE (and Subtitle) Daytime And Nighttime Neutral Wind And Temperature Measurements From Incoherent Scatter Radar At 300KM Over Arecibo		5. TYPE OF REPORT & PERIOD COVERED THESIS/DISSERTATION 6. PERFORMING ORG. REPORT NUMBER
7. AUTHOR(s) Leslie O. Belsma		8. CONTRACT OR GRANT NUMBER(s)
9. PERFORMING ORGANIZATION NAME AND ADDRESS AFIT STUDENT AT: University of Michigan		10. PROGRAM ELEMENT, PROJECT, TASK AREA & WORK UNIT NUMBERS
11. CONTROLLING OFFICE NAME AND ADDRESS AFIT/NR WPAFB OH 45433-6583		12. REPORT DATE 1985 13. NUMBER OF PAGES 34
14. MONITORING AGENCY NAME & ADDRESS(if different from Controlling Office)		15. SECURITY CLASS. (of this report) UNCLASS 15a. DECLASSIFICATION/DOWNGRADING SCHEDULE

16. DISTRIBUTION STATEMENT (of this Report)

APPROVED FOR PUBLIC RELEASE; DISTRIBUTION UNLIMITED

17. DISTRIBUTION STATEMENT (of the abstract entered in Block 20, if different from Report)

18. SUPPLEMENTARY NOTES

APPROVED FOR PUBLIC RELEASE: IAW AFR 190-1

LYNN E. WOLAVER 7/4/86
Dean for Research and
Professional Development
AFIT/NR, WPAFB OH 45433-6583

19 KEY WORDS (Continue on reverse side if necessary and identify by block number)

20 ABSTRACT (Continue on reverse side if necessary and identify by block number)

DD FORM 1 JAN 73 1473 EDITION OF 1 NOV 65 IS OBSOLETE

SECURITY CLASSIFICATION OF THIS PAGE (When Data Entered)

ABSTRACT

Arecibo's twenty acre spherical radar reflector detects the weak electromagnetic energy reflected when pulses are transmitted into the ionosphere. The information contained in this reflected energy reveals the electron temperature, the electron/ion temperature ratio, the line of sight plasma velocity and the electron density among other parameters. This information, combined with neutral densities obtained from the global thermospheric model based on mass spectrometer and incoherent scatter data, MSIS-83, is used to determine the neutral temperature and winds in the F region. This study pertains to the F2 region at a height of 300km over Arecibo (18 N latitude with a magnetic dip angle of 50). A few trends in previous data are noted followed a description of the 300km temperature and neutral wind for daytime and nighttime from 12 days of data, sets of three days from January 1984 and 1985, September 1984, and June, 1984. The experimental neutral temperature is compared to the MSIS model prediction. The observed temperature closely agrees in phase, but averages 50K lower than the model. The observed winds are compared to NCAR's Thermospheric General Circulation Model (TGCM) which has incorporated the effects of tides propagating from the lower atmosphere. The observed winds during equinox agree in phase with the TGCM, but are a factor of three larger in amplitude. The ion drag force is calculated, used to resolve the pressure gradient force, and both are discussed in relation to the observed neutral wind patterns. The pressure gradient force is compared to that predicted by the MSIS model and found to be of comparable magnitude, but often dissimilar in phase.

DAYTIME AND NIGHTTIME NEUTRAL WIND AND TEMPERATURE MEASUREMENTS FROM INCOHERENT SCATTER RADAR AT 300KM OVER ARECIBO

Leslie O. Belsma

December, 1985

Thesis submitted in partial fulfillment of requirements for Master of Science degree in Atmospheric Science at the University of Michigan

ACKNOWLEDGEMENTS

I am especially grateful to Roger Burnside for providing the data and the opportunity for me to carry out this study. Dr. Burnside developed all the software used in the data reduction, generated the plots needed for my final write up, and guided me throughout the project.

I am thankful to those at Arecibo Observatory for enabling me to use the facility and for helping to acquaint me with their computer system.

I am also grateful to Dr. Jim Walker for his patient explanations of various aspects of ionospheric dynamics, for his help in organizing the material, and for his meticulous editing.

INTRODUCTION

The radar detects density fluctuations which for small values of the Debye length, De (=69(Te/N)m, where Te is electron temperature and m is the ion mass), occur as joint longitudinal oscillations of both electrons and ions. When De is much less than the wavelength of the ion oscillations, electrostatic rather than pressure forces dominate the electrons and they follow the ion motion (Walker, 1978). Thus, scattering occurs as if the plasma consisted of particles with the electron temperature and ion mass (Evans, 1974). Incoherent scatter affects only $1x10^{-9}$ of the vertical radar beam and the scattering occurs in all directions; however constructive interference occurs for waves propagating along the direction of the incident radiation with wavelengths equal to 1/2 that of the incident beam, enabling the scattering phenomenon to be observed. The reflected signal travels at the speed c, thus measuring the echo delay determines the height at which the scattering occurs. Characteristics of the reflected spectrum reveal the various F2 parameters.

The electron temperature, Te, is determined from the Doppler broadening of the spectrum, which is less than would be expected from random thermal energy of the electrons because of the presence of ions. The difference in Te and the ion temperature, Ti, is evident in the spectrum shape, giving it a double humped appearance. The plasma wave velocity is proportional to the sum of the ion and electron temperatures, which shifts the spectrum to either side of the transmitted frequency. However, damping from the interaction of the wave's electric field with the charged particles decreases the shift and spreads the spectrum toward the transmitter frequency (Walker, 1978). This damping is proportional to the wave velocity and also, therefore, the electron temperature. The damping is weaker as Te increases and the spectrum has a sharper peak toward the ion wave velocity (ie. the wing of the spectrum increases); more damping occurs for

lower Te and the spectrum is spread more toward transmitter frequency (Walker, 1978). The shift is proportional to the line of sight plasma drift velocity as well as the plasma frequency. Therefore, assuming the ions and electrons move together, the plasma drift can be measured from the spectrum shift. The power of the reflected signal is proportional to the electron density.

TEMPERATURE AND ELECTRON DENSITY

PREVIOUS OBSERVATIONS

In their study of exospheric temperatures over Millstone Hill, Salah and Evans (1973) found that the time of Tmax lags the time of maximum heating, occuring about three hours before thermospheric sunset and that Tmin occurs about two hours before thermospheric sunrise. Tmax occurred at 1530LT in winter, 1600LT at equinox, and 1700LT in summer; Tmin occured at 0400 in winter, 0200 at equinox, and 0030 in summer. The amplitude of the daily oscillation exhibited a seasonal variation with maximium amplitude occuring in summer. They found nightime fluctuations on some days occurring just after midnight with a 50K amplitude and suggested that they could be attributed to an overestimation of temperature resulting from the neglect of frictional heating due to neutral wind. The seasonal variation of the diurnal oscillation is not represented in thermospheric models and is attributed to larger amounts of heat being deposited in the summer auroral zone than the winter (Evans et al., 1978).

In a study of the night-time F2 region over Arecibo based on 19 nights of data during sunspot minimum years, the 400km ion temperatures were found to be slightly higher than model predictions and around midnight remained nearly constant for four hours rather than exhibiting the sinusoidal variation of the Jacchia model (Fukato et al., 1979). Fukato suggests the "flatness" could be due to a semidiurnal oscillation. Thermal equilibrium was established less than one hour after sunset in summer, but three hours following winter sunset. Electron temperatures increased rapidly during summer sunrise, but began increasing two hours before sunrise in winter. The mean midnight temperature was 700K in summmer and 770K in autumn and winter.

In studying night-time conditions during equinox at 350km over

Arecibo, Harper found a 40K ion temperature increase occuring in the three hours after midnight during a time when neutral winds are abating making frictional heating an unlikely explanation (Harper,1973). He suggested that adiabatic heating of neutral gas could cause the temperature increase.

Three nights of data over Arecibo in August 1982 showed the average ion temperature between 300-400km to be around 950K from 2200-0500AST (Burnside, 1984). The study also indicated an average Ti of 875K for three nights in June 1983, 1025K for three January nights in 1981 (solar maximum), and 850K in October 1983.

A 50km drop in the F2 layer height (represented by Zmax) has been observed after midnight followed by a rise at 0400AST at Arecibo (Behnke and Harper, 1973). They found the maximum height of the F2 layer to occur in the early evening. Burnside indicates a seasonal variation in this pattern showing the post-midnight drop/rise to be gradual in June but sudden in Autumn (Burnside, 1981). Harper reports that the peak electron density, N, increases during the midnight drop and mentions a similar Zmax descent pattern in the afternoon (Harper, 1979). Night-time electron densities at the F2 peak over Arecibo presented by Fukato exhibit a seasonal variation in the exponential decay which begins in the late afternoon, the rate being the steepest in the summer and much smaller in the winter (Fukato et al., 1979). An increase in N after midnight appeared as a "small hump" in the decay at 0100 in winter, but only as a decrease in the decay rate from 2200-0100 in summer. He found the exponential decay to continue even after sunrise in summer, but to stop two hours before sunrise in winter with N becoming constant until sunrise. His calculations of Zmax indicated the layer ascending after sunset with the characteristic descent beginning at midnight. Zmax increased before sunrise, with the ascent being concurrent with the time that N ceased to decrease.

CURRENT DATA REDUCTION AND MEASUREMENTS

Roger Burnside takes these measurements by operating the radar in two experimental modes probing the ionosphere from 140 to 540km. Most of the observing time is devoted to transmitting a long pulse (50km) with an 11km spacing. Two heights of the "oversampled" data are then averaged to give 23km spacing and a resolution of about 50km. The antenna is at a 15 degree angle from zenith and is rotated 360 degrees for samplings at 12-18 azimuthal positions which are then averaged for each height to give the electron and ion temperatures. Ion velocity is calculated by assuming no spatial gradient over the horizontal sampling area and fitting a sine wave to the line of sight velocities for the azimuthal angles at each height to resolve the horizontal components (Burnside, 1984).

The ACF data provide measurements of electron density with a 50km resolution, but much more accurate measurements are available from the Barker code data. After every swing through the 18 azimuthal positions a short pulse is transmitted and the Barker coding of the pulse gives a height resolution of 600m. Peak electron densities are calibrated by an on site ionosonde. The Barker measurements are fitted to a Chapman profile using a minimum height between 200 and 250 km and these peak electron densities then compared to the ACF values to eliminate unrealistic temporal increases or decreases in Ne arising when the Chapman profile does not provide a good fit.

In the current study, as in previous experiments, several assumptions are necessary to obtain the neutral temperature at a given height. Ions provide the thermal coupling between electrons and neutrals. The thermal structure is determined by energy from photoionization, thermal conduction and transport. The electron temperature increases as photoelectrons transfer energy to the electron gas. Through elastic collisions between

ions and electrons, the ion temperature increases above that of the neutrals. The difference (Ti-Tn) is usually less than 100K, though neglect of the densities of N 2 and O 2 leads to a slight underestimate of (Ti-Tn) (Salah and Evans, 1973). It is assumed that there is only a single ion species (atomic oxygen) present in the region being studied and that the ions are in thermal energy balance. In using neutral density for a single species from the thermosperic model, atomic oxygen is assumed to obey the laws of diffusive equilibrium. The ACF data directly yield Te, and Te/Ti; Ti is calculated and the neutral density is obtained for the corresponding height and time from MSIS given the 10.2cm flux and magnetic Ap indices. The neutral temperature can be calculated with these parameters using the thermal energy balance equation

$$(1) \quad \frac{(4.82 \times 10^{7})\, N\, (Te - Ti)}{Te^{3/2}} = \frac{0.21\, [O]\, (Ti + Tn)^{1/2}}{(Ti - Tn)}$$

where [O] is the atomic oxygen density. Next it is assumed that the temperatures vary linearly with height and using a linear fit for Te, Ti, and Tn for seven heights in January and June of 1984 from 285-424km and for ten heights in September 1984 and January 1985 from 262-470km, the three temperatures for the given altitude of 300km are calculated.

The neutral temperatures from this study are shown in Figures 1A-D. Mean temperatures in the current data set are considerably less than those calculated at Arecibo during and in the years just after solar maximum. Burnside (1984) found the highest average night-time temperatures in June; the same is true of this study. The latest MSIS model incorporates the "flatness" which Fukato demonstrated and though it matches the data more closely than a sinsusoidal variation of earlier models would, it does not reflect small amplitude, short time scale oscillations

which occur overnight at Arecibo. Harper noted a 40K temperature increase between midnight and 3am; a similar pattern occurs in the data, only 3 hours earlier.

In all four sets of data in the current study, ion temperatures reach peak values between 1700-1800AST. The difference between Ti and Te never exceeds 100K. In June and September, the ions and neutrals are in thermal equilibrium from 1900-0500AST, while in January equilibrium is approached more gradually and lasts from 2100 to only 0300. The neutral temperature pattern reflected in the data agrees well with MSIS predictions though the timing of the peak temperature often varies by an hour or two. The model consistently predicts temperatures 40 to 80K higher than observed with the largest differences occurring in the afternoon. After midnight the model indicates a very gradual temperature decrease to a minimum, but temperature maxima interrupt this period of cooling in the data sets.

The overnight equilibrium temperature in January 1984 averages 725K, then Ti begins to rise above Tn by 0300AST. Again, the evening cooling trend is interrupted by a 50K increase from 21-2300, with a leveling off or another peak at 2am before dropping to Tmin at 3am. Tn begins rising after 0500, with a sharp increase after 9am to a peak of 900K by noon, not cooling until after 1700. Figure 1C shows that MSIS neutral temperatures average about 50K warmer with 80K differences at the extrema and no indication of the accelerated temperature increase in the late morning.

The average night-time temperature a year later (and closer to solar minimum) in January 1985 is 650K with Tn reaching a peak of 825K at 1700 but averaging only about 750K in the afternoon. The measured temperatures average about the same as MSIS from 1900-0900, but the predicted temperatures are 80K higher in the daytime with a peak at 1600 when it is observed closer to

1800AST. As in January 1984, the ion temperature begins to exceed the neutral just after 3am. A well defined temperature increase is not evident after 2100AST and a rapid drop occurs from 0130-0300, followed by an increase from 0300-0500 which is not reflected in the MSIS model (see Figure 1D).

The average Tn throughout the night in the September 1984 data set is 650K and as in June, Ti is equal to Tn from 1930-0530. Except from September 19-20 when temperatures drop to minimum at midnight and begin rising steadily two hours later, the temperature increase from 21-2300 is evident, though of less amplitude than in June, and a more gradual bulge also occurs around 3am (see Figure 1B). During the day Tn reaches a peak of 850K with Ti averaging about 30K warmer. MSIS predicts daytime neutral temperatures 40K higher than observed indicating maximum Tn at 1700.

For three June 1984 nights, the average night-time (22-05AST) neutral temperature at 300km is 750K, with ions and neutrals in equilibrium from 1930- 0530. Tn falls off quickly after the late afternoon peak, but a 50K increase disrupts the cooling trend from 2100-2300 and again from 0200-0400. During the day, Ti is about 50K warmer than Tn. An unusually rapid heating is evident on June 27 when Tn increases rapidly from 05-07am to 850K and 975K at 1700. This sharp increase does not occur on the previous morning. MSIS indicates a slightly larger temporal gradient in the morning and the phase of temperature oscillation matches the data. However, MSIS temperatures average about 70K higher (see Figure 1D).

Figures 2A-D show the electron densities at the F2 peak and the height of the layer peak. In January, 1984, the electron density is the highest in the morning when the height of the layer is the lowest (between 210 and 240km). The peak densities occur in the afternoon around 6pm in the other three data sets.

In January, 1985 and September, 1984, the afternoon density maximum coincides with an F2 layer drop. In June, the layer stays around 300km throughout the day. In all four data sets, the F2 peak reaches is highest altitude around midnight and then undergoes a rapid 100km drop, followed by a rise or leveling off by 3am. This post midnight drop and rise is consistent with previous observations (Behnke and Harper, 1973) though a significant seasonal variation is not evident. An abrupt rise and fall of the F2 peak height occurs after midnight on September 19 when the magnetic Ap index jumped to 36 up from 3 on the previous day.

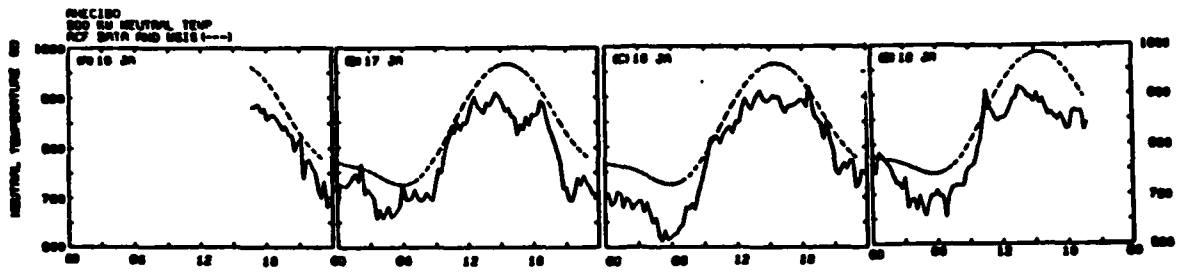

Figure 1A. Tn increases before and after midnight on Jan 17, but just a leveling off occurs on the 18th. Rapid heating before noon.

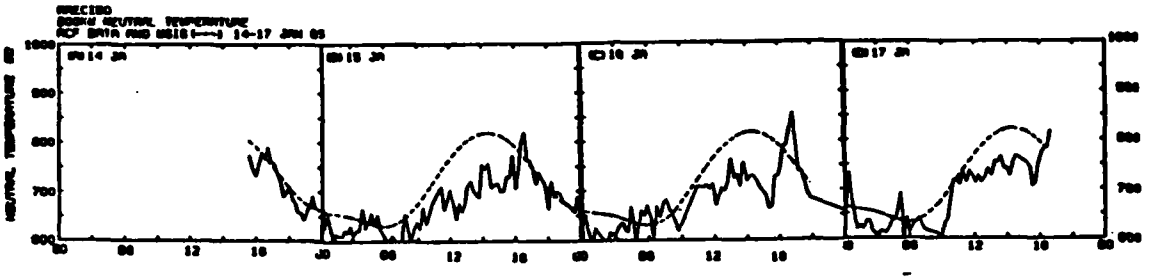

Figure 1B. Average Tn lower than in 1984. Maximum Tn occurs 2-3 hours later than the peak in the MSIS curve. Temperature increase at 3am.

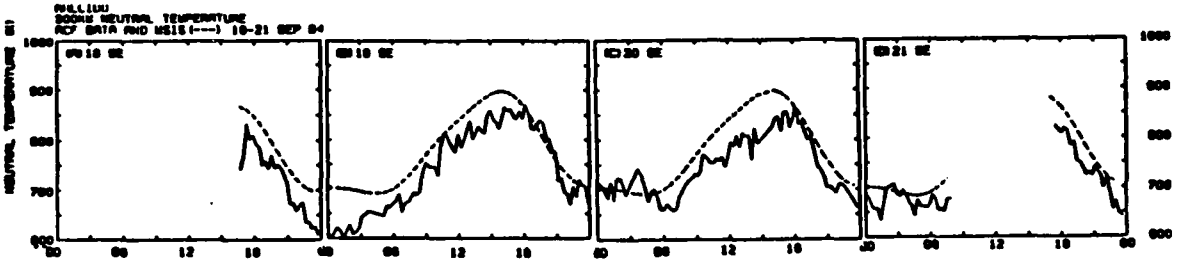

Figure 1C. A 40K Tn increase 2-3 hours before midnight and again at 3am. Maximum Tn occurs an hour later than model prediction.

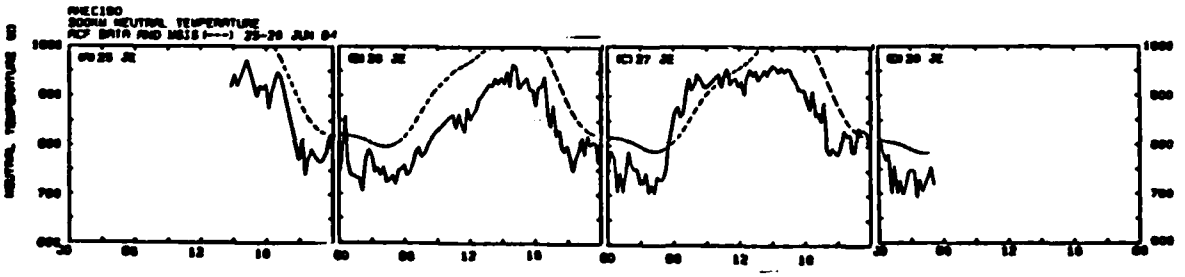

Figure 1D. Rapid heating on Jun 27. MSIS indicates a slightly steeper gradient in the morning.

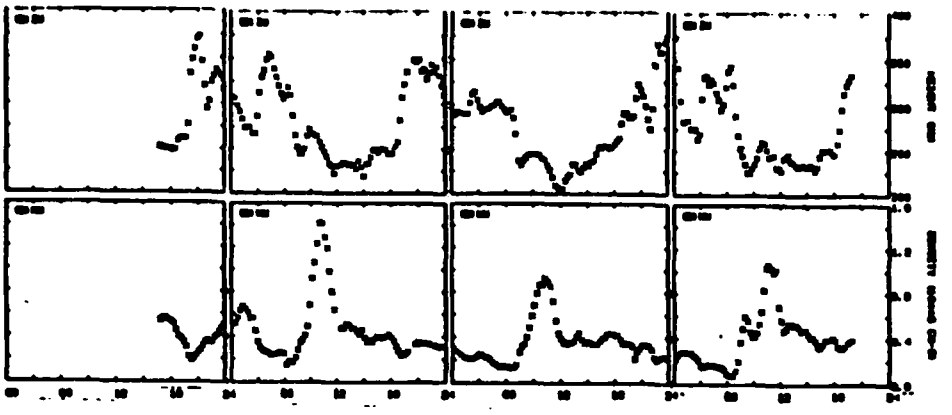

Figure 2A. Height and density of the F2 peak from 16-19 Jan, 1984. Highest densitiy occurs just before noon.

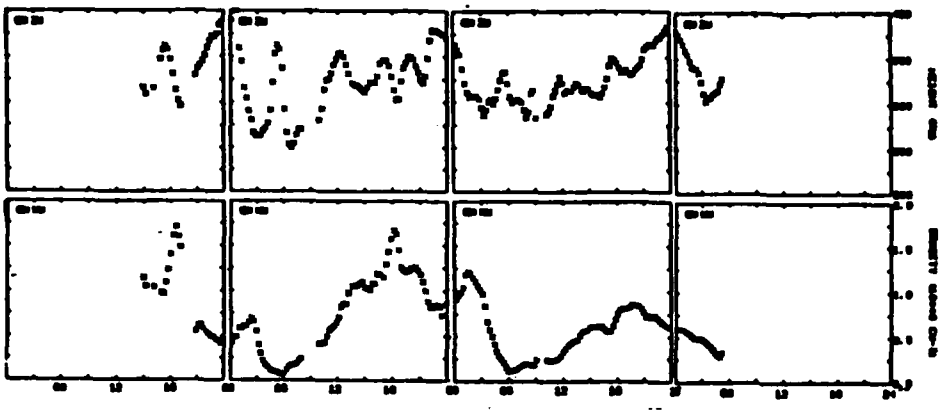

Figure 2B. The same for 14-17 Jan, 1985. Maximum density in the afternoon.

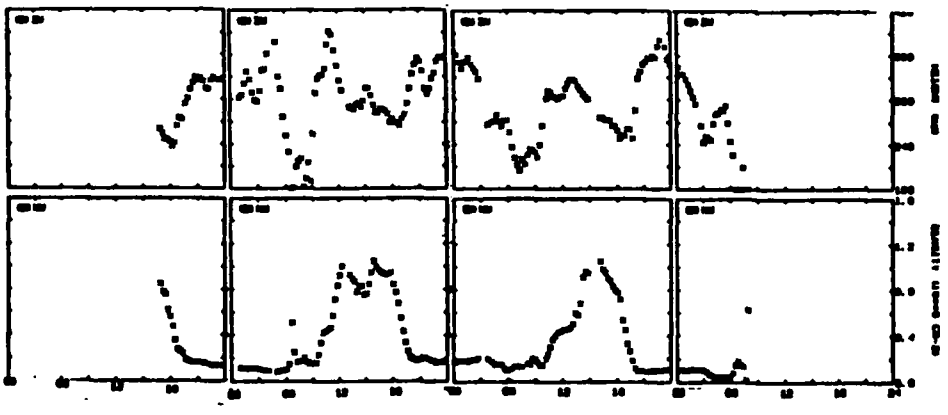

Figure 2C. The same for 24-27 Sept, 1984. Maximum peak density in the afternoon corresponding to a collapse in the layer height.

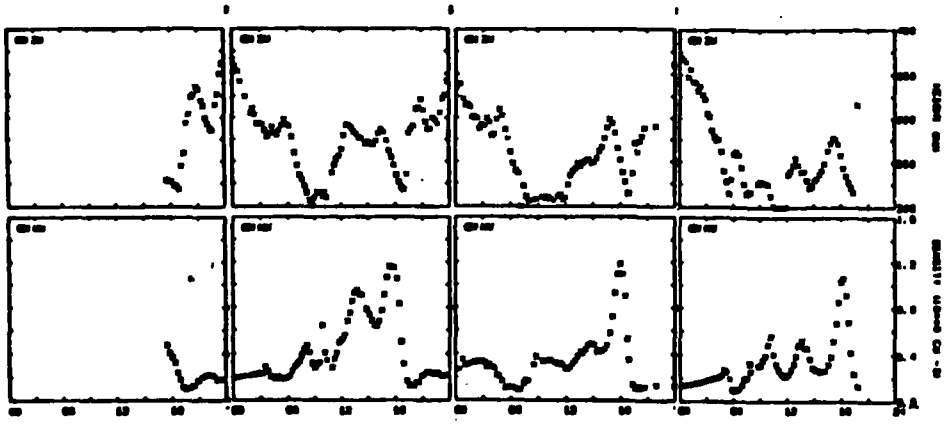

Figure 2D. The same for 24-27 Jun, 1984.

NEUTRAL WIND

PREVIOUS OBSERVATIONS

Amayenc and Vasseur determined day and night neutral winds using the same experimental methods as the current study and found stronger flow to the poles in the winter, the effect of transequatorial flow from summer to winter hemisphere (Amayenc, 1971). They measured ion drifts and temperature gradients at various F2 levels with the St Santin-Nancay radar and, with neutral densities from the Jacchia and Slowey model, they determined the diffusion velocity thus inferring the neutral velocity. The meridional winds were presented for two days in 1969 and one in 1968, characteristic of low magnetic activity. They found poleward winds from 7am to 8pm in winter reaching a maximum velocity of 100m/s. In summer, the poleward flow did not exceed 50m/s and reversed to equatorward earlier in the day (around 3pm). The same phase occurred during equinox as in summer, but the maximum poleward velocity was 80m/s. The southward flow in winter approached a 200m/s peak abruptly after the evening reversal in winter, but the equatorward flow increased more gradually to a 200m/s peak in summer. The maximum equatorward velocity during equinox was about 120m/s.

Using the same analysis technique as the current study, Behnke and Harper (1972) determined meridional neutral winds for daytime on January 8 and October 31, 1971 and for five winter nights at Arecibo in 1970. They found poleward flow throughout both days with maximum poleward flow in mid-morning. The poleward flow maximum was 140m/s in January and the average around 60m/s. The strongest poleward flow during equinox was 60m/s with an average of 35m/s. Assuming a steady state, Behnke and Harper determined the October 31 pressure gradient as the force balancing the ion drag term. The gradient was positive (poleward) all day with a 2cm/s2 peak at 10am and a 3cm/s2 peak at 2pm. They explain the

morning flow in the same direction as the pressure gradient as a result of electric field effects where a 30m/s poleward perpendicular ion velocity, V-perp, adds 40m/s to poleward flow and 20m/s southward V-perp adds 25m/s southward component to the neutral wind in the afternoon. Looking at the five winter nights, Behnke and Harper found northward winds up to 80m/s in the early evening reversing by 10pm with an equatorward maximum of 80m/s two hours later. Southward flow abated becoming zero or poleward again by 2am and averaging slighly poleward through the early morning.

Harper determined the meridional neutral winds at Arecibo for four nights in March 1971 from 5pm to 5am (Harper, 1972). An average poleward flow of 35m/s occurred in early evening reversing at 10pm as in winter. The equatorward winds climbed to 120m/s around 11pm and dropped to zero three hours later becoming briefly northward but oscillating about zero for the remainder of the early morning. Harper determined that the F-layer achieved its maximum height coincident with the maximum equatorward neutral winds.

Burnside (1983) determined average wind contours from 250-490km using Arecibo incoherent scatter data for nighttime hours during solar maximum. Averages for data in December 1981, February 1982, and April 1982 indicate southward winds above 300km and weak northward below (an average of nine nights in June 1980 and August 1982, does not reflect this pattern). The equatorward flow at the higher levels is especially apparent during a magnetic event. The plot for a magnetically disturbed night on 28-29 December shows southward velocities exceeding 200m/s above 370km but less than 25m/s below 300km (Burnside et al., 1983).

CURRENT DATA REDUCTION AND MEASUREMENTS

As previously mentioned the line of sight velocity is obtained from the spectrum shift. The components are resolved as functions of altitude assuming no horizontal spatial gradient over the area covered as the antenna rotates and no temporal changes in the time for one rotation (about 20 minutes). Given calculated neutral temperatures, neutral densities, [O] and [N2], are obtained from MSIS and the diffusion velocity in the direction of the earth's magnetic field is calculated using the O+ diffusion equation (Burnside et al., 1983):

$$(2) \quad Vdiff = (-Da)\sin I \left[1/Hp + 1/N(dN/dz) + w/Tr(dTr/dz) + 1/Tp(dTp/dz)\right];$$

where: Reduced T: $Tr = (Ti+Tn)/2$; Plasma T: $Tp = (Ti+Te)/2$;

$$w = 0.37 \text{(thermal diffusion factor)};$$

$$Da = (3.02\times10^{17})Tn^{1/2} / A[O]+19.9[N^2](Tn^{1/2});$$

$$A = 1.08 - 0.14 \log Tn + 0.0045 (\log Tn)^{1/2}$$

The gradient in electron density at 300km is obtained from the Chapman fits to the Barker code density measurements above 200km. Error occurs in determining the height and density of the peak when the layer drops below 200km, but calculations of the vertical density gradient at 300km with the F2 peak far below should not be significantly affected.

The component of the neutral wind along the magnetic field line is taken to be the difference between the ion parallel velocity, Vpa, and the diffusion velocity. Therefore, in the horizontal meridional direction, neglecting the vertical component of the neutral wind (Burnside,1984):

$$(3) \qquad Ux = (Vpa - Vdiff)/\cos I$$

The calculated neutral temperature rather than model calculations of T-infinity are used to get the most accurate neutral densities from MSIS (Burnside, 1984). However, realizing possible error due to local variations in density which are not reflected in model profiles, the effect of changing [O] by a factor of two on the wind calculations has been examined. In Figure 3, neutral wind calculated with MSIS [O] is compared to that using MSIS [O]x2 (which halves the diffusion velocity). The amplitude of the equatorward flow is damped (by up to 80m/s at velocity peaks) while that of the poleward flow is slightly increased, but the direction of flow (or the neutral wind pattern) is not significantly altered. The calculated error for the experimental neutral wind ranges from 0 to 30m/s averaging around 16m/s or +8m/s. The error bars are included in the plots of neutral winds.

The ion drag term, FID, is defined as the difference between the neutral wind and the ion velocity in the x direction times the collision frequency, vni (=Kni(N), where Kni=8x10@-8 is the O+,O collision parameter). Substituting for the neutral wind from the expression above:

$$(4) \qquad FID = -[8x10^{-8}(N)/\cos I](Vdiff - Vz\sin I)$$

The local acceleration of the meridional neutral wind, Uxt, is calculated by fitting a cubic to three adjacent measurements. Then, the net southward pressure gradient force, Fx, is calculated from the momentum equation where the coriolis force, the advection term, and the viscous drag are neglected. Given these approximations (discussed by Burnside, 1984):

$$(5) \qquad Fx = Uxt + FID$$

Neutral wind results from the four data sets are shown in Figure 4. Some general trends are common to all four data sets. Maximum equatorward winds (positive Ux) usually occur between 2300-0100AST. Steep acceleration and deceleration surround this peak. Winds drop off or become poleward by 0300 followed by southward acceleration until 0500. The daily minimum or most poleward winds occur around noon (except for a poleward maximum at 6pm in January 1985), otherwise oscillating about zero until late afternoon when poleward flow occurs briefly before a rapid equatorward acceleration to the diurnal maximum in southward flow. This last trend toward equatorward flow is interrupted by a one hour poleward acceleration at 9pm which is much more noticeable in the winter data, causing 100-150m/s drop in equatorward flow before the midnight maximum in equatorward flow is reached.

The experimental pressure gradient force, Fx, is shown in Figure 5. In all four data sets, the equatorward pressure gradient force is strongest in the late evening and the strongest in the poleward direction around sunrise near equinox and in late morning during winter solstice. (An equatorward (poleward) pressure gradient force, Fx, implies a northward (southward) pressure gradient.) A poleward gradient force is sometimes observed late in the afternoon, but from noon to sunset the gradient force is usually weak. The neutral wind exhibits the same pattern as the pressure gradient force except during periods of high electron densities in the afternoon when the ion drag force prevents the wind from responding to the gradient.

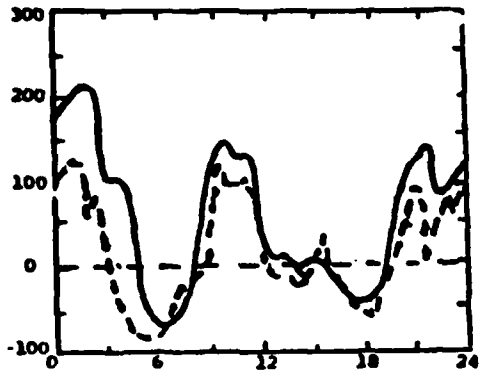

Figure 3. Hand smoothed plots of experimental neutral wind for 19 Sept, 1984 to demonstrate sensitivity to atomic oxygen density; positive southward. Solid line is the result using MSIS [O], dashed using 2 x MSIS [O].

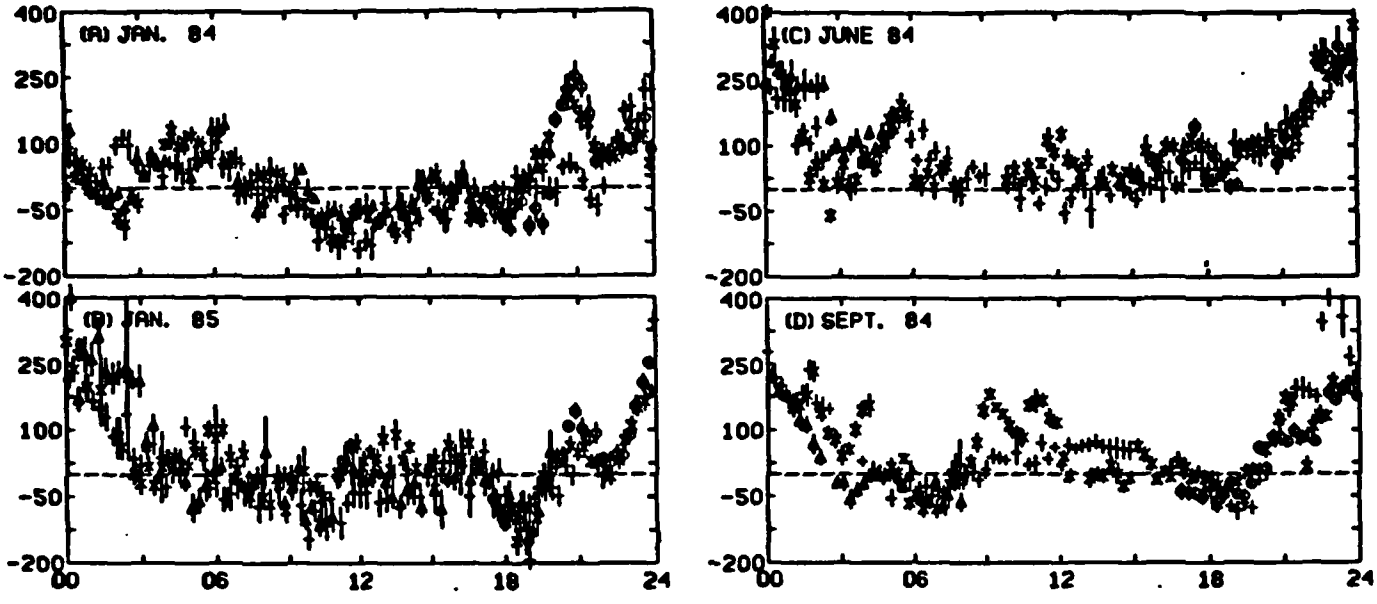

Figure 4. Observed neutral winds for the four data sets; positive equatorward.

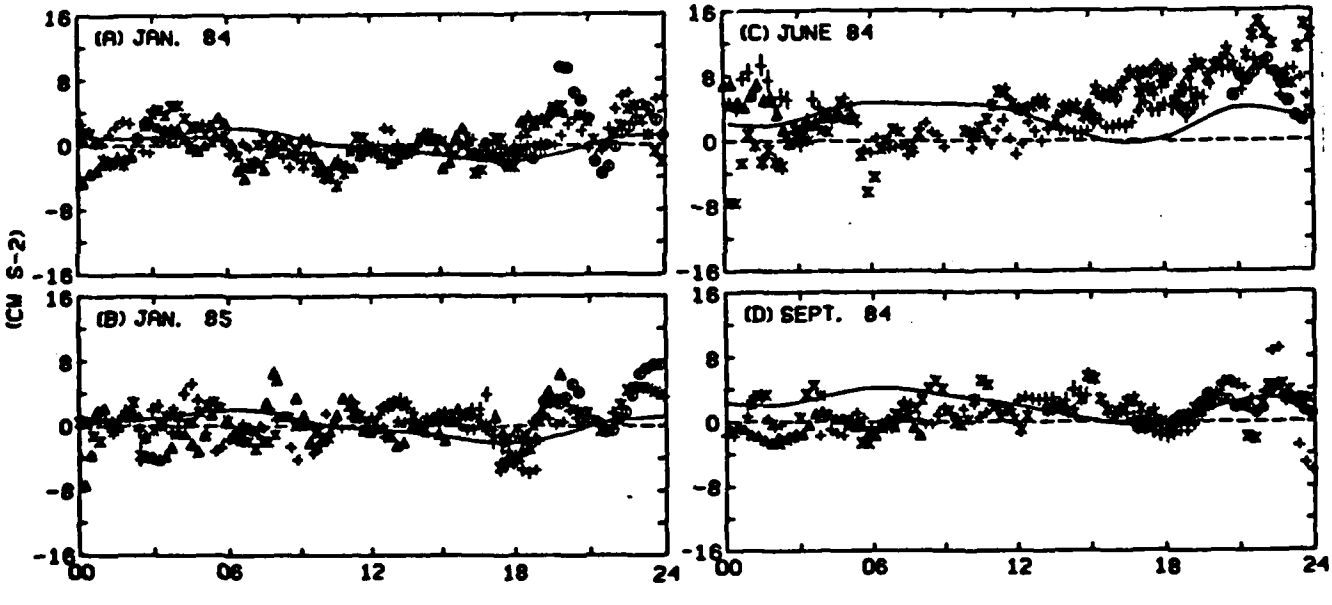

Figure 5. Observed pressure gradient force, Fx. A positive Fx corresponds to a poleward gradient in pressure (or an equatorward force).

In January 1984, the neutral wind is equatorward at midnight up to 200m/s and begins decelerating steadily reversing to poleward flow at 2am (see Figure 6A). On January 12, this postmidnight abatement is interrupted by a sudden equatorward acceleration to 100m/s southward flow at 3am. Looking back at Zmax, it is apparent that the layer height did not exhibit the postmidnight drop/rise pattern found on the other nights (Figure 2B). For the other January 1984 data, poleward flow occurs briefly at 3am with maximum values of -125m/s before Ux reverses again and climbs to a second equatorward peak of 150m/s just before sunrise. In January 1985, the velocity at midnight reaches 325m/s (400 on the 17th) which is the diurnal maximum, and more day to day variation exists in phase and amplitude (Figure 7A). The postmidnight poleward flow occurs between 3-5am and is less than -25m/s, the second equatorward peak is 100m/s and occurs at 5 or 6am, or not at all. In January 1984, by 8am, the equatorward wind has subsided and the flow reverses again with the diurnal maximum in poleward flow (125m/s) occurring at noon. In January 1985, the flow becomes poleward between 6-7am and reaches a poleward maximum of -125m/s but returns to an average around zero by noon which lasts until 5pm when a sudden poleward acceleration causes the strongest poleward flow of the day, -175m/s at 7pm followed by equatorward acceleration. However, after noon in 1984, rather than a zero average velocity, the poleward velocity just drops gradually during the day and no afternoon peak in poleward flow occurs before a sudden equatorward acceleration which begins at 6pm, rather than 7pm. In both January 1984 and 1985, a peak in equtorward wind occurs at 9pm and is always followed by 100-150m/s drop before climbing to the midnight peak equatorward flow which is the diurnal maximum in 1985 (as in the June and September data sets). In 1984, however the strongest daily winds occur with the peak in equatorward flow at 9pm.

The pressure gradient force in January is southward (northward

pressure gradient) from 2am, when the wind reverses from poleward to equatorward flow, to 6am. (January 17, 1985 is an exception in that a strong poleward gradient occurs at 3am.) The pressure gradient and ion drag forces, Fx and FID, for January 1984 and 1985 are shown in Figures 7B,C and 8B,C. The resisting ion drag is weakly positive as electron density is less during this time and the wind responds to the pressure gradient. The effect of electron density on FID is apparent in comparing 4am on January 17 to January 19, 1984. The pressure force is stronger on the 17th, but Ux is 150m/s on both nights. The wind is not larger on the 17th because the ion drag force is a factor of two larger on the 17th. (Though electron density at the peak does not differ significantly on the 17th from the 19th, the perpendicular ion velocity is greater on the 19th in the north and upward direction contributing to the larger resisting ion drag force.) The average pressure gradient force in January 1984 is zero by sunrise becoming northward with a -5cm/sec)2(peak between 10-11am, an hour before the neutral wind peaks in the poleward direction. Though the pattern varies more rapidly during this time in January 1985, Fx is generally poleward with an earlier peak at 9am. In January 1984, an incrase in the ion drag between 10-11am reflects the electron density which, as noted earlier, is highest in the morning rather than the afternoon for this data set. The pressure force averages around zero in the afternoon, becoming poleward before reversing to equatorward at 6pm. In January 1984, the force becomes only slightly poleward before reversing, but in 1985, a very strong poleward Fx occurs from 5-6pm driving the observed northward neutral winds. As happens in the morning in January 1984, the ion drag increases in the afternoon coincident with maximum electron density, and when the densities decrease, an increased FID reflects increased neutral winds. In both 1984 and 1985, a southward peak up to 6cm/s2 occurs at 8pm with the force dropping off to zero or even slightly negative by 9pm and climbing again to a second southward peak force at 10pm. The wind exhibits the same pattern with roughly a one hour time lag.

After the 10pm peak in pressure gradient, the force drops of rapidly preceeding the rapid deceleration of Ux.

Neutral wind plots for the September, 1984, data are shown in Figure 8A. The neutral winds are the strongest at midnight in September, 1984, and reverse to weak poleward flow at 3am, subsiding to zero and then accelerating poleward again, reaching 100m/s northward between 6-7am. As noted earlier, Septmber 19 is a magnetically active day and the winds undergo a sudden equatorward acceleration resulting in a 175m/s southward velocity between 10am and noon, but the wind averages around zero from noon to sunset, rather than poleward flow which occurs thoughout the afternoon in winter. Moreover, on the other September day, after the morning poleward velocity subsides and reverses at 9am, the flow averages 75m/s equatorward until 5pm. The wind then reverses and poleward flow (up to 100m/s) occurs from 5-9pm. This poleward reversal in the afternoon is also evident, though less pronounced, on the magnetically active day. All September data indicate equatorward acceleration in the evening which subsides at 10pm, but increases again to the strong equatorward flow (250m/s) observed around midnight (400m/s is observed on September 20).

From Figure 8B it is evident that the experimental pressure gradient in September exhibits the same pattern as the neutral winds from sunset to sunrise, shifted an hour earlier, as in the winter data. (The wind lags Fx by three hours after midnight, September 20 though the measured ion drag force, FID, is not unusually large.) The maximum equatorward pressure force occurs at 10-11pm. Fx is poleward at 3am, 6am, and again around 6pm. A strong equatorward gradient force occurs in the afternoon (3pm), but does not drive a strong acceleration in the neutral wind because of high ion drag resulting from maximum electron density at the F2 peak.

Immediately noticable in Figure 9C is that the June experimental neutral winds are almost always equatorward. Though there is deceleration at sunset, there is not a reversal to poleward wind before climbing to the diurnal maximum in equatorward flow (300m/s) at midnight. As in the other data sets, the wind falls off rapidly after midnight, but again, in June, they do not reverse at 3am. Strong equatorward winds (175m/s) are observed at 6am followed by rapid deceleration to zero in the morning, but not reversing. On one June day, -50m/s occurs around noon and Ux averages slightly poleward until 5pm, but an average 50m/s equatorward occurs on the other June afternoon.

The experimental equatorward pressure gradient force is often a factor of two larger in June than in the other data sets (Figure 9B). The diurnal peak force at 10pm is 10 to 16cm/s 2. A poleward force is dominant from midnight to sunrise on June 26, though the post midnight period on the other two June data days is characterized by a weakening equatorward force. Fx is weakly poleward from sunrise to noon on June 27 concurrent with the only poleward winds observed in June. Though an equatorward gradient persists past midnight on June 26 and again on June 27, Ux begins decelerating at midnight due to the high ion drag force (FID=13cm/s 2 at 1am June 27 corresponds to unusually high peak electron density).

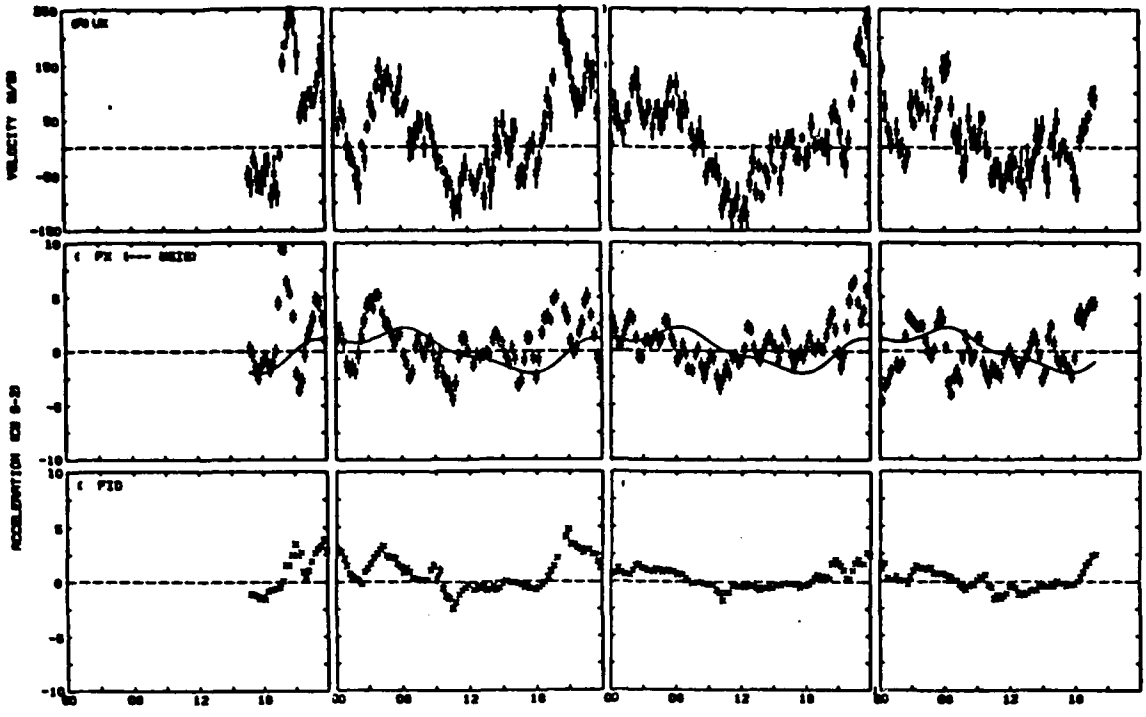

Figure 6. Neutral wind, Ux, pressure gradient force, Fx, and ion drag force, FID, for 16-19 Jan 1984.

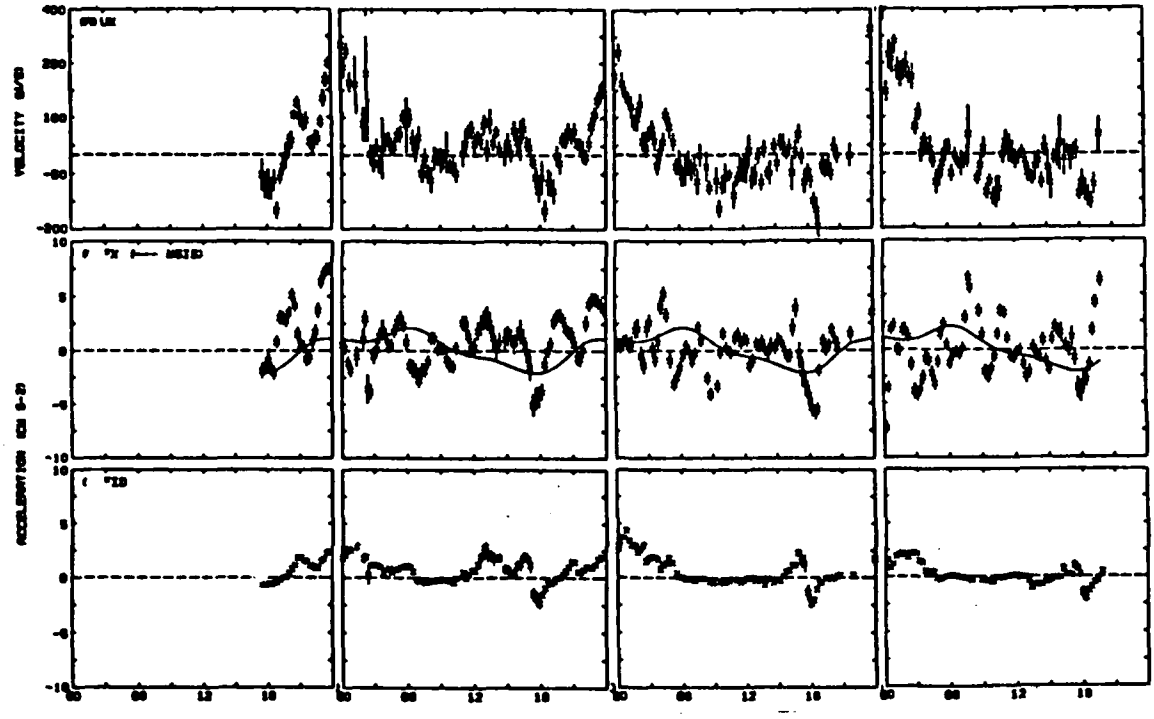

Figure 7. Ux, Fx, and FID for 14-17 Jan 1985.

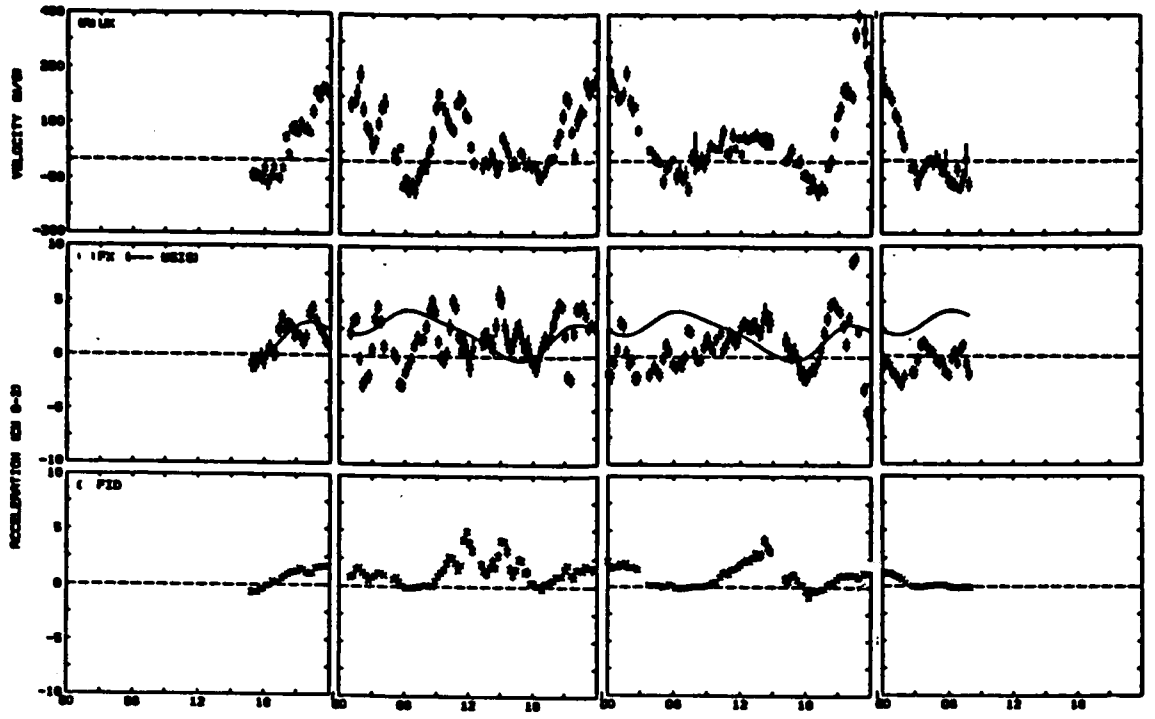

Figure 8. Neutral wind, Ux, pressure gradient force, Fx, and ion drag force, FID, September 18-21, 1984.

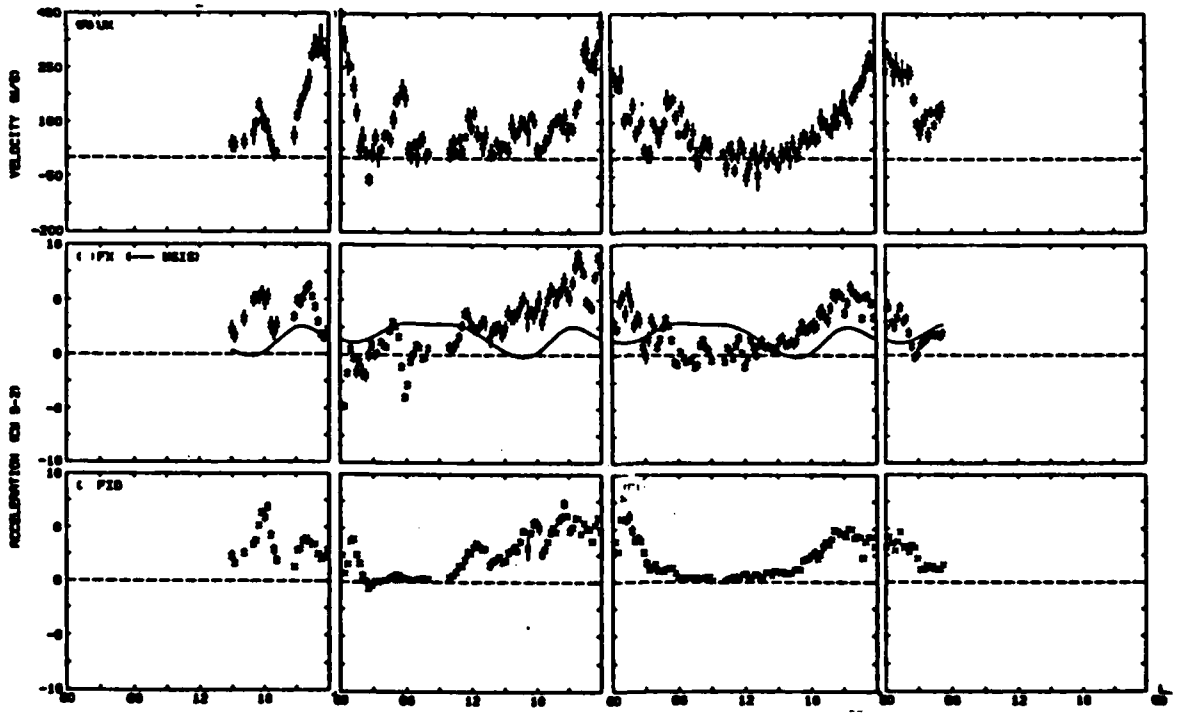

Figure 9. Ux, Fx, and FID for 25 to 28 Jun 1984.

The neutral wind observations from this study show some similarities to those from previous observations dicussed earlier. The magnitudes are larger for the current study. The maximum neutral wind late in the evening is usually around 250m/s equatorward while Harper found the equatorward velocity maximum at 11pm to be 120m/s. Wind measurements from St Santin-Nancay (40 N lat) bear more resemblance with maximum equatorward winds of 200m/s in winter and summer evenings. Amayenc found the peak equatorward wind at equinox to be almost 1/3 less (120m/s); no such seasonal difference is evident in the current data. Harper found maximum poleward flow to occur at 10am (October data) and though it occurs at this time in the January 1984 data, poleward flow in September is strongest around sunrise and again sunset. Harper determined a flow reversal from equatorward to poleward at 2am, a phenomenon which is observed at 2-3am in this study.

Looking back at Figures 2A-D, it is evident that the January 1984 data are unique in that the maximum electron density of the F2 peak occurs just before noon. The neutral wind and ion velocity patterns can help explain this phenomenon. The layer height is low from noon to sunset. More recombination is occuring in the afternoon, reducing afternoon peak densities. Vertical ion velocity, Vz for January 1984 averages around zero or weakly upward until noon when downward motion begins and persists until late evening. On the other data sets, downward ion velocity is not observed until after 6pm. This behavior of Vz presumably causes the observed lower Zmax and therefore the peak density pattern. The ion velocity perpendicular to the magnetic field lines can contribute to the vertical ion velocity. For this January 1984 case, V-perp peaks in the north/up direction late in the morning and at noon begins to reverse to the south and downward direction with a -60m/s peak velocity around 3pm and an average velocity in this direction until after sunset. Only a west electric field can drive this component of the plasma motion. The perpendicular and vertical ion velocities for

January 19, 1984 are shown in Figure 10 and are representative of the other January 1984 data. Earlier observations of daytime periods at Arecibo have shown a south/downward V-perp in the afternoons implying a west electric field (Behnke and Harper, 1973). Only electric fields can drive ions perpendicular to the magnetic field, but the neutral wind can contribute to the vertical ion velocity. The neutral wind in January 1984 accelerates steadily after 9am to -125m/s by noon. Velocities drop off gradually but an average poleward flow of -50m/s lasts through most of the afternoon. Though poleward velocity reaches 125m/s by 10am in January 1985, the average velocity from noon to sunset in January 1985 is around zero, and slightly equatorward in the June data. The poleward flow in the afternoon in January 1984 pushes ions down the field lines contributing to the downward vertical ion velocity. Therefore, downward Vz dominates thoughout the afternoon and recombination on the F2 bottomside occurs more rapidly suppressing the afternoon peak density.

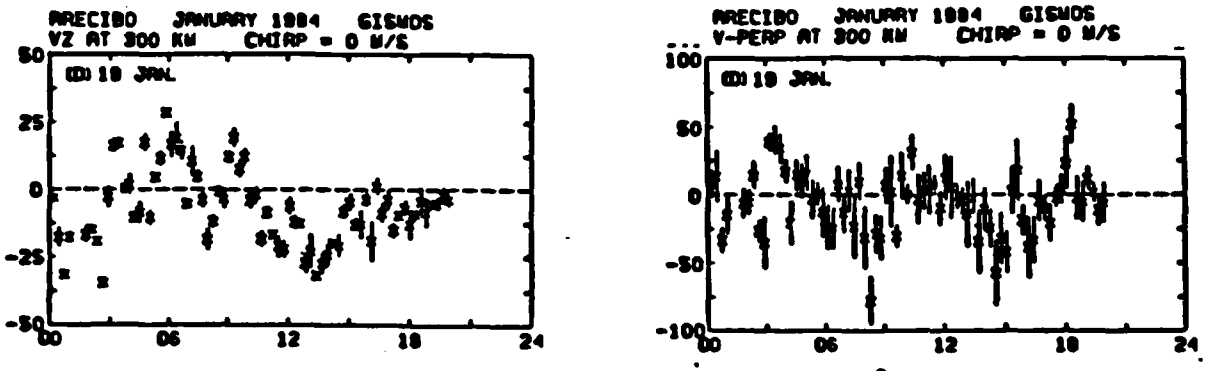

Figure 10. Vertical ion velocity, Vz, (positive up, cm/s^2) and perpendicular ion velocity, V-PERP (positive up and poleward, m/s^2) for 19 Jan 1984.

COMPARISON BETWEEN DATA AND MODELS

The meridional pressure gradient predicted by the MSIS-83 model atmosphere is calculated by taking the north-south difference in predicted temperature and density. The model force is represented by the solid line in the plots of the pressure gradient force for the four data sets in Figures 6C,7C,8C, and 9C. The experimental and predicted forces (proportional to minus the pressure gradient) are of the same order of magnitude, in the range of +10cm/s2, though phases often differ. In all four data sets, both model and observation indicate a peak in the equatorward pressure gradient force two or three hours before midnight, though two peaks are observed in the winter evening. The model consistently predicts the most poleward gradient force (or minimum equatorward force) around 6pm while it is observed in the late morning (except for the afternoon peak in the poleward force in January 1985). MSIS maintains a negative gradient force from noon to 10pm which appears only briefly before sunset in the data. The calculated Fx matches the model better in phase during the evening in June and September than in winter.

In January, the observed pressure gradient force has a southward peak at 45am. The MSIS predicted pressure force peaks in the southward direction at 7am (see Figures 6C,7C). Both observation and MSIS indicate the force becoming more northward during the morning. However, observed values peak northward around 10am (in January 1985 the pattern is varied but a north pressure force dominates from 6-10am) and average around zero throughout the day while MSIS indicates that the pressure force continues to increase negatively to a maximum northward force at 6pm. In both observation and MSIS, the gradient force becomes southward in the early evening. The experimental force changes to southward at 7pm and quickly reaches a peak by 8pm at which time the model force is just becoming positive (southward). The observed gradient force then drops rapidly to zero (or even reverses) but

quickly rises again to a second southward peak at 10pm. This pattern is not evident in the model which continiues slowly rising to a very weak amplitude maximum just before midnight.

In winter the predicted equatorward gradient force weakens around sunrise to become poleward by late morning, remaining poleward until 10 at night. The only poleward gradient force predicted in June and September is from 3-6 in the afternoon. In observation, Fx is poleward in September briefly from 5-6pm but, in June, Fx is equatorward and increasing during the afternoon and evening. The MSIS force matches the experimental Fx in the evening of both June and September in that peak equatorward force occurs around 9pm. MSIS predicts a southward force with minimum values in the hours after midnight and increasing to a maximum value at 5am which in June, is predicted to last until noon and, in September, to decrease very gradually. After midnight, on two of the three June nights, the observed equatorward gradient force increases when MSIS predicts a minimum (a minimum is observed on the other June night). Similarly in September, Fx has a southward peak during the model prediction for a minimum. However,a smoothed curve for the September data would have a minimum (actually poleward Fx) one hour later than the model minimum (the latter being a weak equatorward force). The most marked difference between the data and the model is that the observed Fx is zero or negative (poleward) when MSIS indicates a maximum positive (equatorward) force around sunrise and the data begins to increase positively as the model becomes more negative. Thus the phase of the observed pressure force is opposite the model from sunrise to 3pm in September and to 6pm in June.

Dickinson discusses NCAR's Thermospheric General Circulation Model, TGCM, predictions of the flow for 100 to 500km indicating circulation on constant pressure surfaces at 150 and 300km (Dickinson, 1984). Absorption of UV and EUV radiation as well as auroral heat input are used as energy sources with an average

solar F10.7cm flux of 68 representing equinox during solar minimum conditions. Coincident geographic and geomagnetic poles are assumed in this version of the model (denoted here as TGCM-1). At 300km, neutral winds are shown to blow equatorward up to 80m/s from 1800 to 0600. A slight northward component develops after sunrise but drops off just after noon. Acceleration is mostly in the zonal direction until early evening. Velocities are more than 1/3 less at 150km blowing southward only from 8pm to midnight. A meridional acceleration does not occur until 9am when winds become northward up to 25m/s dropping off by 4pm. Where only a slight poleward component to the flow develops in the morning at the upper level, a dominant north acceleration persists throughout the day at 150km. Conversely, the equatorward acceleration is more persistent at 300 km. Figure 11 is taken from the published results of this model.

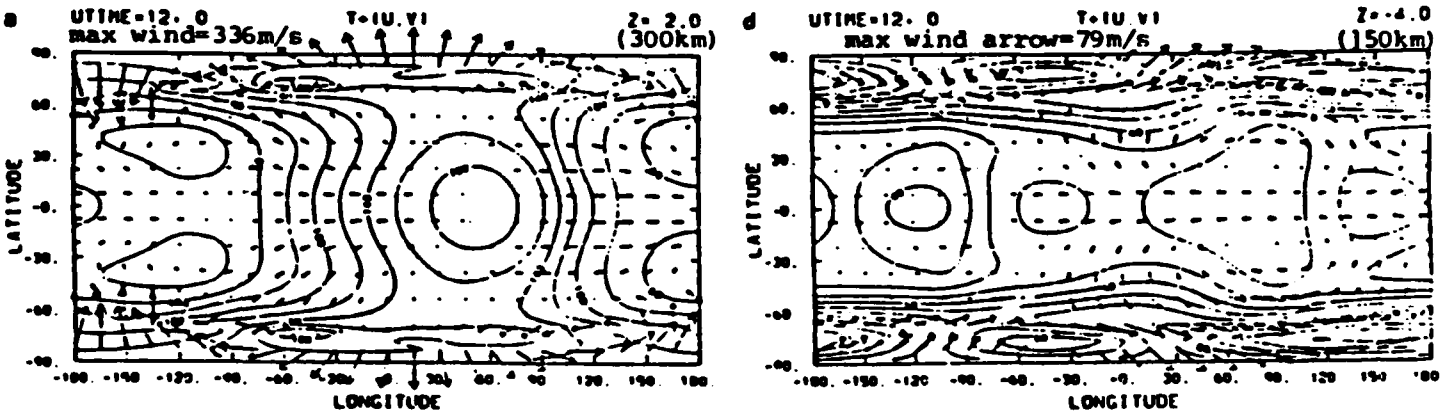

Figure 11. 1983 TGCM prediction for equinox during solar minimum. 1200UT corresponds to 0800AST. Equatorward flow is more pronounced at 300km; poleward at 150km. (Dickinson,1984)

Tim Killeen has analysed TGCM including high latitude and in situ heating and assuming separate geographic and geomagnetic poles. His analysis (denoted here as TGCM-2) determines among other parameters, predicted neutral winds specifically for Arecibo. Another generation of TGCM by Casandra Fesen (referred to here as TGCM-3) produces vertical cross sections of velocity fields for Arecibo assuming coincident geographic and geomagnetic

poles, excluding high latitude heating, and excluding or including the effects of tidal propogation from below the thermosphere (the most recent model development). Model results are shown in Figure 12A for solar maximum equinox. The experimental winds are in geomagnetic coordinates. The geomagnetic coordinates are plotted to emphasize differences in the model run with separate geographic and geomagnetic poles and that assuming coincident poles (for which geographic coordinates are plotted). Difference in these two plots also arises from different type graphs used to draw each and to a less extent from excluding high latitude heating from the TGCM-3 analysis. At 300km, in geomagnetic coordinates, poleward flow is indicated during the day from 7am to 2pm with a 45m/s peak at 9am. The flow is southward throughout the rest of the 24 hour period reaching a maximum of 45m/s at 3am. The geographic poleward flow begins an hour earlier and lasts four hours longer in the afternoon and the magnitude of the peak equatorward velocity is reduced by a half. One might keep in mind these differences in comparing observation to the remaining model plots which are all in geographic cordinates. The tidal effects contribute to the duration of the poleward meridional flow, shifting the maximum poleward flow to the afternoon rather then in the late morning but with little change in magnitude. The magnitude of the equatorward velocity nearly doubles from that without tide effects, but the duration of the equatorward flow is reduced, lasting only from 7pm to 3am.

Various TGCM results for solar minimum equinox are shown in Figure 12B. The TGCM-1 prediction is derived from the global map in Figure 11 by taking longitude to be equivalent to a time scale and measuring the meridional wind component over Arecibo. Another plot in Figure 12B was drawn from a vertical cross section produced from TGCM-3 without tides. The trend in the neutral wind from these model results is for poleward flow beginning at 4am, reaching a maximum in late morning (~45m/s) and decreasing in the afternoon reversing to equatorward around 5pm.

The predicted peak equatorward velocity is at midnight, and though the recent model only indicates peak speeds of 25m/s, in geomagnetic coordinates, the predicted maximum would be greater. Also included in Figure 12B is a plot drawn from the vertical cross section at Arecibo from TGCM-3 wiht the effects of tides propagating from below included. The poleward flow begins earlier (2am) and peaks at 4am and 5pm with magnitude comparable to that for the peak poleward flow predicted to occur in the late morning by modeling without tides. The equatorward velocities are doubled with the peak predicted to occur an hour before midnight.

The experimental neutral winds for the four September, 1984 days characterize solar minimum equinox for a comparison between theory and observation (Figure 13B). (The model uses F10.7=80 and the September observations are for F10.7=100.) The phase of the September winds matches the theoretical plot which includes tidal effects (solid line in Figure 12B); however, observed amplitudes are a factor of three larger. The maximum predicted equatorward winds are 65m/s while peak observed winds are usually 250m/s (400m/s has been observed). The strongest equatorward flow is at midnight in both theory and observation, though the theory calls for peak poleward flow at 3am and though poleward flow is observed at that time, stronger poleward flow is observed at 7am.

The TGCM-2 prediction (with the high latitude heating and separate poles) has also been analysed for Arecibo for winter solstice solar maximum conditions (Figure 12C). The model indicates poleward flow all day and night except for two hours around 3am when the meridional wind drops to zero or 10m/s southward.

The observations of neutral wind in January 1984, just following winter solstice and two and a half years after solar maximum, show little similarity in phase to theory, and model

winds are always poleward, while except for a brief post-midnight reversal, the observed winds are equatorward from sunset to sunrise (Figure 13A). The peak in equatorward winds observed at 6am could correspond to the theoretical minimum poleward flow indicated two hours earlier. Similarly, a maximum in poleward flow is predicted at 8am, but observed at noon. A maximum in poleward wind is evident at 6pm in both theory and observation. Though the model poleward wind decelerates in the evening, theory does not indicate the maximum equatorward wind observed at 8pm and again at midnight.

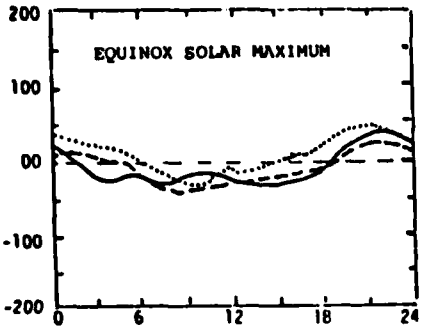

Figure 12A. Dotted: TGCM-2 (geom. coords.)
Dashed: TGCM-3, without tides
Solid: TGCM-3, with tides

For reference to Figures 12A-C (also see text):

TGCM-1: (Dickinson) Model includes high latitude and in situ heating, coincident geog/geom poles. Plot drawn from global map in Figure 11.

TGCM-2: (Killeen) Model includes high latitude and in situ heating, separate geog/geom poles. Plots drawn from graphs of Ux vs time at Arecibo.

TGCM-3: (Fesen) Model includes in situ heating, coincident geog/geom poles, with/without tides. Plots drawn from vertical cross sections of contours of Ux in time.

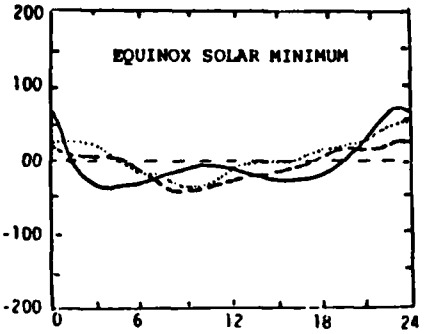

Figure 12B. Dotted: TGCM-2
Dashed: TGCM-3, without tides
Solid: TGCM-3, with tides

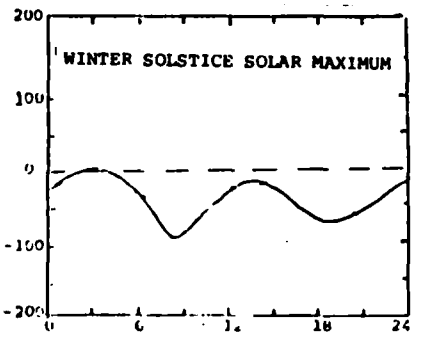

Figure 12C. TGCM-3 (geom coords.)

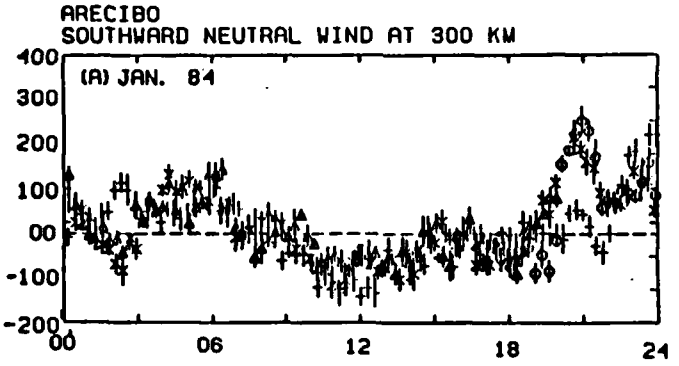

Figure 13A. January 1984 observations to characterize winter solstice two years before solar minimum. The model results are for winter solstice solar maximum and do not include effects of tides propogating from below (Fig 12C) and show little similarity to these observations.

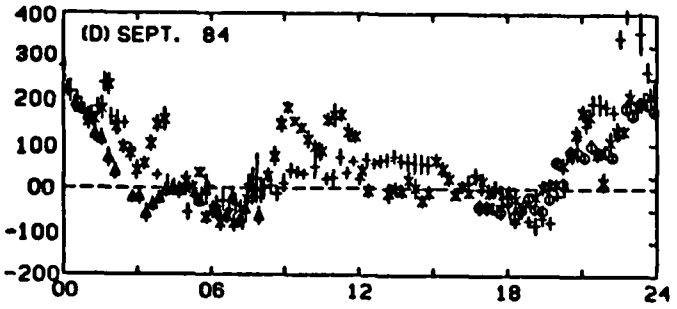

Figure 13B. September 1984 observations characterize equinox solar minimum and can be compared to the solid line in Fig 12B. The phase in theory is similar to observation, but the observed amplitude is a factor of three larger and there is an equatorward shift of the zeroline.

The tendency toward equatorward winds at Arecibo in the present data might be related to a Hadley cell circulation driven by high latitude heating in which a return poleward flow occurs at lower levels. The previously mentioned wind contours for Arecibo during solar maximum showed predominantly equatorward flow above and poleward flow below 300km (Burnside et al., 1983). Global maps from TGCM for the constant pressure surfaces at 150 and 300km also show more pronounced northward flow at the lower level with more southward flow aloft (Dickinson, 1983). Mayr discusses a Hadley cell circulation with the upper branch having poleward flow (Mayr et al., 1984). He suggests that with solar differential heating at low latitudes, temperature, and pressure decrease toward the poles causing a Hadley cell. The redistribution resulting from wind induced diffusion depletes the atomic oxygen concentration at the low latitudes thus possibly reversing the pressure gradient (cf.Mayr et al., 1984).

Early determinations of thermospheric wind speed from analysis of changes in satellite orbit inclinations indicated a mean eastward zonal wind of about 130m/s at 300km for 30 latitude (King-Hele et al., 1970). This would result in a component of 18m/s in the magnetic south direction over Arecibo, but is not enough to explain differences in TGCM predictions and the current observations. In addition, theoretical models produce much smaller values of mean zonal winds supported by mass spectrometer measurements from Dynamics Explorer II (Mayr et al., 1984).

The observed temperatures agree well with MSIS in both phase and amplitude. However, although the observed pressure force is of the same magnitude as that predicted by MSIS, the phases are significantly different. Rishbeth (1977) determined that a more complex pressure distribution than the Jacchia model then being used would be necessary to explain Arecibo nightime winds.

Perhaps MSIS can not reproduce small scale dynamics influencing the equatorial tropical wind field. Rishbeth describes a tropical high, a diurnal bulge in the pressure field from which diverging wind would give a poleward flow at Arecibo. He suggests that a displacement of this high would result in transequatorial flow and, therefore, for a high situated north of Arecibo, an equatorward flow component.

The TGCM underestimates the amplitude of the neutral wind observed in this study. The inclusion of high latitude heating and separate geomagnetic and geographic poles in the model used for comparison would increase the predicted amplitude some, but not nearly by a factor of three. The neutral winds in this study are deduced from the measured parallel ion velocity and the calculated diffusion velocity. The magnitude V-par is consistent with previous results (<100m/s); the diffusion velocity is generating the large neutral winds observed. The sensitivity of the neutral wind to atomic oxygen density has been demonstrated. If the densities predicted by MSIS are too small, through the diffusion coeficient, V-Diff and therefore Ux will be too large, though again, not by a factor of three. On the other hand, the TGCM model could be overestimating electron density and therefore overestimating ion drag resulting in smaller winds. In addition to bringing the phase in close agreement with observation, the inclusion of tides propagating from below the thermosphere increases the neutral wind amplitude. The forcing term for the semidiurnal tidal modes used is tuned to observations at Arecibo which, as noted previously, are much less than those observed in this study.

Acknowledgement: The Arecibo Observatory is operated by Cornell University under contract with the National Science Foundation.

BIBLIOGRAPHY

Amayenc,P. and Vasseur,G., Neutral winds deduced from incoherent scatter observations and their interpretation, J. Atmos. Terr. Phys., 34, 351-364, 1972.

Behnke,R., and Harper,R., Vector measurements of F region ion transport at Arecibo, J. Geophys. Res., 78, 8222-8234, 1973.

Behnke,R., Kelley,M., Gonzales,C., and Larson,M., Dynamics of the Arecibo iono sphere: A case study approach, J. Geophys. Res., 90, 4448-4452, 1985.

Burnside,R., Benhke,R., and Walker,J., Meridional neutral winds in the thermoshpere at Arecibo: Simultaneous incoherrent scatter and airglow observations, J. Geophys. Res., 88, 3181-3189, 1983.

Burnside,R., Dynamics of the low-latitude thermosphere and ionosphere, Tech. Rep., Natl. Sci. Found.,1984.

Dickenson,R., Ridley,E., and Roble,R., A three-dimensional model of the thermosphere, J. Geophys. Res., 86, 1499-1512, 1981.

Dickenson,R., Ridley,E., and Roble,R., Thermospheric general circulation with coupled dynamics and composition, J. Atmos. Sci., 41, 1983.

Dougherty, J., On the influence of horizontal motion of the neutral air on the diffusion equation of the F-region, J. Atmos. Terr. Phys., 20, 167-176, 1960.

Evans,J. Incoherent scatter sounding, J. Atmos. Terr. Phys., 36, 2183-2234, 1974.

Evans,J. A review of F-region dynamics, Rev. Geophys. and Spa. Phys., 13, 887-921, 1975.

Evans,J. Oliver,W.,Jr., and Salah,J., Thermospheric properties as deduced from incoherent scatter measurements, J. Atmos. Terr. Phys., 41, 259-278, 1977.

Fukato,S., Sato,T., Kimura,I., and Harper,R., Seasonal mean structure of the night-time F2 region over Arecibo, J. Atmos. Terr. Phys., 41, 1205-1221, 1979.

Harper,R., Nighttime meridional neutral winds near 350km at low to mid-latitudes, J. Atmos. and Terr. Phys., 2023-2034, 1973.

Harper,R., A semidiurnal tide in the meridional wind at F-region heights at low latitudes, J. Geophys. Res., 84, 411-415, 1979.

Hedin, A., A revised thermospheric model based on mass spectrometer and incoherent scatterdata: MSIS-83, J. Geophys. Res., 88, 10170-10180, 1983.

Mayr,H., Harris,A, Hedin,E., Spencer,N., and Wharton,L., Thermospheric superrotation revisited, J. Geophys. Res., 89, 5613-5624, 1984.

Rishbeth,H., On the theory of diffusion in the ionosphere, Geophys. J.R.Astr. Soc., 41, 311-317, 1975.

Rishbeth, H., Dynamics of the equatorial F-region, J. Atmos. Terr. Phys., 39, 1159-1168, 1977.

Rishbeth, H., Ganguly,S., Walker,J.C., Feild-aligned and field-perpendicular velocities inthe ionospheric F2-layer, J. Atmos. Terr. Phys., 40, 767-784, 1977.

Rishbeth, H., Ion-drag effects in the thermosphere, J. Atmos. Terr. Phys., 41, 885-894, 1978.

Rishbeth, The F-region dynamo, J. Atmos. Terr. Phys., 43, 387-392, 1981.

Roble, R.G., Emery, B.A., Salah, J.E., Hays, P.B., Diurnal variation of the neutral thermospheric winds determined from incoherent scatter radar data, J. Geophys. Res., 79, 1974.

Salah, J.E., Evans, J.V., Measurements of thermospheric temperatures by incoherent scatter radar, Space Res. XIII, 268-286, 1973.

Salah, J.E., Holt, J.M., Midlatitude thermospheric winds form incoherent scatter radar and theory, Radio Sci., 9, 301-313, 1974.

Walker, J.C.G., Space science without rockets: measurement of ionospheric properties at the arecibo observatory, EOS, 59, 180-189, 1978.

Walker, J.C.G., Radar measurements of the upper atmosphere, Science, 206,1979.

END

FILMED

5-86

DTIC